

Raman-Active modes in Homogeneous and Inhomogeneous Bundle of Single-Walled Carbon Nanotubes

K. Sbai, A. Rahmani, H. chadli and J. L. Sauvajol*

Equipe de Physique Informatique & Modélisation des Systèmes, Université MY Ismail, Faculté des Sciences, BP 11201, Zitoune, 50000 Meknès, Morocco.

** Laboratoire des Colloïdes, Verres et Nanomatériaux (UMR CNRS 5587), Université Montpellier II, 34095 Montpellier Cedex 5, France.*

In the present work, the non-resonant Raman active modes were calculated for several diameters, chiralities and sizes for homogeneous and inhomogeneous bundles of single-walled carbon nanotubes (BSWCNT's), using the spectral moment's method (SMM). Additional intense Raman active modes are present in the breathing-like modes (BLM) spectra of these systems in comparison with a single fully symmetric A_{1g} mode characteristic of isolated nanotubes (SWCNT's). The dependence of the frequency of these modes in terms of diameters, lengths and number of tubes is investigated. We find that for finite bundle, additional breathing-like modes (BLM's) appear as a specific signature. Finally, the effects of the inhomogeneous bundles on the Raman spectra were studied.

Corresponding Author: email kh.sbai@yahoo.fr

Keywords: Nanotube, non-resonant Raman, Raman spectroscopy, spectral moment method.

I. INTRODUCTION

Since the discovery of carbon nanotubes in 1991 [1], the attention of both experimentalists and theoreticians has focused on their properties. In particular, SWCNT have currently been intensively investigated worldwide for their intrinsic one-dimensional properties and their promising applications. Among the techniques extensively used to characterize these materials, Raman scattering plays a preponderant role [2]. The Raman spectrum of SWCNT is dominated below 500 cm^{-1} by the radial breathing modes (RBM) and in the high frequency region, between 1400 cm^{-1} and 1600 cm^{-1} , by the tangential modes (TM). The assignment of the band below 500 cm^{-1} was carried out using the results of force-constant of the lattice dynamics of isolated nanotubes [3, 4], tight-binding [5, 6, 7] and ab-initio [8, 9, 10] calculations for the zone-center phonons, and a bond-polarizability model [4] for the Raman intensity. Raman studies have shown that the radial-breathing mode in the low frequency region shows a straightforward dependence on the diameter of the SWCNT that can be used to determine the distribution of tube diameters [4, 11]. The TM shape depends strongly on whether the tube is metallic or semi-conducting [12, 13, 14]. In the intermediate frequency range, $600\text{--}1300\text{ cm}^{-1}$, the intensity of the Raman spectrum is weak, several peaks were observed, but their assignment is a controversial matter [15, 16, 17, 18].

In main production methods available today, the produced SWCNT's are formed as a polydisperse mixture with various diameters and chiralities. So, the direct comparison between theory and experiment is difficult because of the wide range of diameters and chiralities usually present in the samples. The analysis of Raman data

recorded using theoretical models based on infinite tubes has been frequently applied as a tool to analyze the SWCNT mean diameter and diameter distribution in both bulk and nanoscopic samples. In Raman analysis of SWCNT bundles (BWCNT's), the exact strength of the intertube interaction within a bundle is still unknown. From previous studies, this intertube interaction has induced an upshift of the RBM of about $8\text{--}12\text{ cm}^{-1}$. However, one has to be aware that the finite length and number of tubes forming bundle have to be included in the detailed analysis.

In a recent paper [19], by using the spectral moment's method in the framework of the bond-polarization theory, we have calculated the polarized Raman spectra of chiral and achiral SWCNT's as a function of their diameter and length. An investigation of finite-size effects was extended to large finite lengths up to 85 nm as well as to achiral and chiral tubes of several diameters. The dependence of tangential modes on chirality and the dependence of the Raman spectrum on the tube length were clearly observed.

In this work, we study the Raman spectra of single-wall carbon nanotube bundles in the framework of the polarizability theory. Their dependence on the diameters, lengths, chiralities and the number of (identical or different) tubes in the bundle is investigated.

II. MODEL AND METHOD

Let us recall that the ideal nanotube structure can be obtained from graphene sheet by rolling it up along the straight line connecting two lattice points into a seamless cylinder in such a way that the two points coincide [4]. Following the usual terminology of reference [3], the tube can be specified by integers (n, m) that define the

translation vector between the two points. Alternatively, the tube can be described by its diameter D and the chiral angle θ which is the angle between the tube circumference and the nearest zigzag of carbon-carbon bonds. The tube is called achiral for $\theta=0^\circ$ (zigzag type) and $\theta=30^\circ$ (armchair type), and chiral for $0^\circ < \theta < 30^\circ$.

The diameter D of a single-wall carbon nanotube is given by

$$D = a \frac{\sqrt{3(n^2 + m^2 + nm)}}{\pi}$$

with $a=0.142$ nm.

When SWCNT's are closely packed together, a three dimensional carbon bundle is formed. From the diffraction profile of the crystalline ropes of SWCNT, it has been previously reported that these systems can be represented by two dimensional infinite hexagonal lattices of uniform cylinders [20]. For finite-size bundle, the nanotubes were placed parallel one to each others on a finite-size hexagonal array of cell parameter $a_0=D_t + d_{t-t}$, where d_{t-t} represent the intertube spacing. The intertube interaction energy is minimised in respect to the intertube separation and the angle of simultaneous rotation of all tubes about their axes. The optimized intertube separations are roughly equal to 0.32 nm. This value, slightly smaller than the inter-graphene sheets distance in graphite, is in agreement with calculations [21, 22] and experiments [23]. The number of tubes per bundle is called NT.

In the present work, we calculate the polarized Raman spectra for finite and infinite bundle. The C-C intratube interactions are described by using the same force constants set than the one used in our calculations of the Raman spectra of isolated SWCNTs [19] and formally introduced by Saito [11]. A Lennard-Jones

potential, $U_{LJ} = 4\epsilon \left[\left(\frac{\sigma}{R} \right)^{12} - \left(\frac{\sigma}{R} \right)^6 \right]$, is used

to describe the Van Der Waals intertube interactions between the tubes in bundle, with parameters $\epsilon=2.964$ meV and $\sigma=0.3407$ nm [19, 30]. These values have recently been found to describe correctly the Van Der Waals contribution to the C_{60} bulk cohesive energy [27, 28].

In the SWCNT's Raman study, we use the non-resonant bond-polarizability model [29] to describe the coupling between vibrational modes and photons. By the way for SWCNT bundles, we neglect the lattice effect on the bond-polarizability model parameters.

A usual method to calculate the Raman spectrum requires, besides the polarization parameters, the eigenvalues and the eigenvectors which can be obtained by direct diagonalization of the dynamical matrix of the system. However when the system contains a large number of atoms, as for long finite SWCNT bundles, the dynamical matrix is very large and its diagonalization fails or requires

long computing time. By contrast, the spectral moment's method allows us to compute directly the Raman spectrum of very large harmonic systems without any diagonalization of the dynamical matrix [19, 24, 25]. Otherwise, for small samples, both approaches lead exactly to the same position and intensity for the different peaks.

III. RESULTS AND DISCUSSION

Using the spectral moment's method, the Raman active-mode frequencies are directly obtained from the position of the peaks in the calculated Raman spectra. The line shape of each peak is assumed to be Lorentzian and the line width is fixed at 1.7 cm^{-1} . The intensity of the Raman spectrum is normalized in respect to the number of carbon in the sample under consideration. In our calculations, the axes of the tubes are along the Z axis, and carbon atoms of each tube are along the X axis of the SWCNT reference frame. The laser beam is kept along the y axis of the reference frame. We consider that both incident and scattered polarizations are along the z axis to calculate the polarized ZZ spectra. More than 50000 atoms in carbon nanotubes were treated.

A. Infinite homogeneous BWCNT's

Firstly, the calculations are performed on infinitely homogeneous bundles (crystal) of SWCNT's of several diameters. We recall that infinite SWCNT's are obtained by applying periodic conditions on unit cells of the studied nanotubes. The results for typical armchair tubes (9, 9), (12, 12), (15, 15), (18, 18) and (21, 21) are reported in Figure 1, where the ZZ Raman spectra are displayed in the BLM (on the left) and TLM (on the right) regions. In the TLM region, all spectra display the peaks corresponding to A_{1g} modes. Shifts for A_{1g} modes are observed when the tube diameter increases. In the BLM region, the ZZ spectra exhibit two peaks denoted here as RBLM (for radial breathing-like mode) and BBLM (for bundle breathing-like mode). The comparison between the Raman spectra of the SWCNT's and BWCNT's shows the appearance of a second mode (BBLM) at a frequency higher than that of RBLM one. For all modes, we observe a downshift with increasing tube diameter. One can see that for small nanotube diameters, only the RBLM has an important intensity, and this mode is associated with a nearly pure breathing like eigenvector. This RBLM mode is the mode that has been reported in different studies [5, 6, 26]. For diameter larger than 1.4 nm, the eigenvector of RBLM shows a clear hexagonal deformation due to intertube interactions. As a consequence, the upshift of RBLM becomes less important and, even for $D > 2.0$ nm, the RBLM mode has a frequency lower than the RBM frequency of SWCNT. At the same time, the higher frequency mode BBLM becomes more and more intense.

B. Finite homogeneous BWCNT's

To study effects of finite size on homogeneous BWCNT Raman-active modes, we developed calculations of Raman spectra of bundles of different number of infinite nanotubes. In figure 2, we report the ZZ polarized Raman spectra for a typical (9, 9) armchair BWCNT's for four numbers of tubes $NT = 1, 7, 19$ and 91 in comparison with the crystal system. Firstly, we observe that the TLM region is slightly affected by the increase of NT . From $NT=1$ to crystal, the frequency of the A_{1g} mode passes from 1585 cm^{-1} to 1586 cm^{-1} . Concerning the BLM region, the ZZ spectrum shows, besides the A_{1g} shift from 183 cm^{-1} for SWCNT to 204 cm^{-1} for infinite BWCNT, additional peaks around the A_{1g} frequency mode for given finite values of NT . For example, for $NT = 19$, two additional peaks are observed at frequencies 195 and 209 cm^{-1} . The more the size of the beam increases, the more the additional peaks around A_{1g} are grouped together to form the single peak around 204 cm^{-1} for an infinite beam. We note the presence of the BBLM around the frequency 300 cm^{-1} for all values of $NT > 1$.

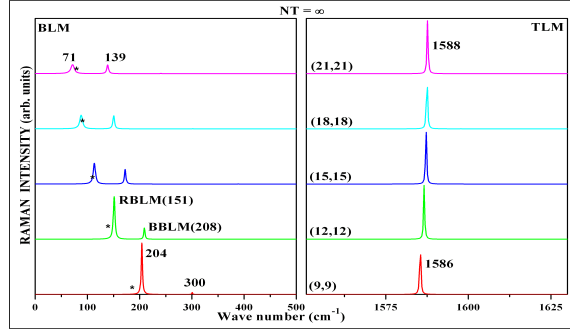


Fig. 1: The ZZ calculated Raman spectra of (n, n) SWCNT crystals for $n=9, 12, 15, 18$ and 21 from bottom to top. The stars give the position of the RBM of isolated tubes.

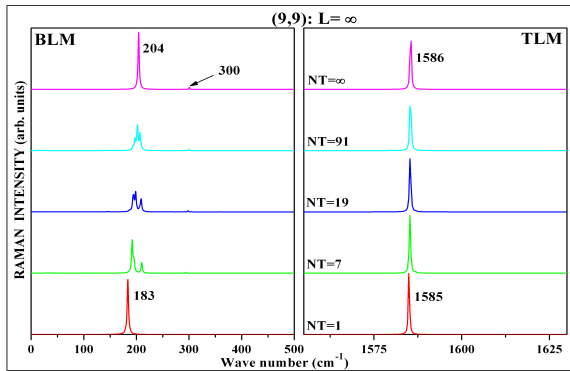


Fig. 2: The calculated ZZ Raman spectra of finite size $(9, 9)$ BWCNT's as a function of the number of tubes in the bundle: $NT=1, 7, 19, 91$ and crystal from bottom to top.

C. Inhomogeneous finite bundles of infinite SWCNT's

Previously, we have studied the vibrational structure of bundle of identical tubes. But the present production techniques could lead to the formation of bundles constituted by tubes not

necessarily with the same diameter or chirality. In this section we are interested in the effect of inhomogeneous finite bundles of SWCNT's, formed with infinite tubes of different diameters.

Firstly, the calculations are performed on finite bundles of identical infinitely long ($L = \infty$) SWCNT's of several diameters. The results of a typical armchair system formed with two infinite tubes with different diameters $((9, 9)@(n, n))$ are reported in Figure 3 where the ZZ Raman spectra are displayed in the BLM (on the left) and TLM (on the right) regions. The behaviour of the modes in the TLM region is the same as in homogeneous system with two A_{1g} modes around 1585 cm^{-1} corresponding to the SWCNT's $(9, 9)$ and (n, n) . In the BLM region, the ZZ spectra exhibit additional peaks denoted here as BM_N in comparison with homogeneous system. From Fig. 3 we can conclude that the lower frequency pair of the peaks (modes BM_3 and BM_4) can be mainly related to a vibration of larger tubes and that higher frequency peaks can be associated to a vibration of the $(9, 9)$ tube. We noted here that the mode BM_1 (around 204 cm^{-1}), found in a $(9, 9)$ homogeneous bundles, is observed in all case. We observe a splitting of the RBM mode of the larger tube into two components (down and up shifts) in particular for $(12, 12)$ and $(18, 18)$. This demonstrates that in such a case the experimental spectra would allow us to prove that the individual components of the bundle even if the modes are split.

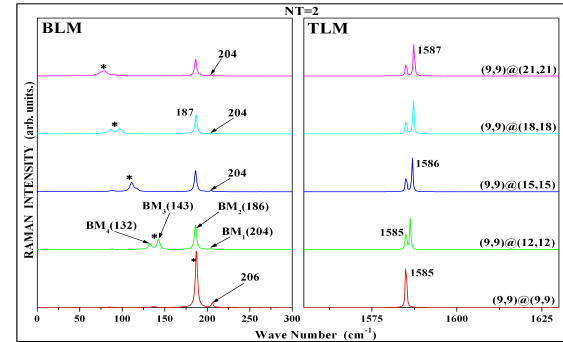


Fig. 3: the ZZ calculated Raman spectra of inhomogeneous finite BWCNT's, formed with two SWCNT's of different diameters: $(9, 9)@(n, n)$, for $n=9, 12, 15, 18$ and 21 (from the bottom to top), in BLM (in the left) and TLM (in the right) ranges. The stars indicate the position of the RBM mode of isolated tubes.

Secondly, in order to show the chirality of SWCNT effects on the bundle, we reported in Figure 4 the results of Raman spectra of inhomogeneous finite bundles of SWCNT's, formed with two infinite tubes, approximately of the same diameters and different chiralities. In the TLM region, the observed modes are close to those found in homogeneous system with two A_{1g} active-modes. In the BLM region, the ZZ spectra exhibit additional peaks in comparison with homogenous

system. Particularly for $(9, 9)@(16, 0)$, we observe a strong splitting of the RBM modes into several modes (downshifts and up shifts).

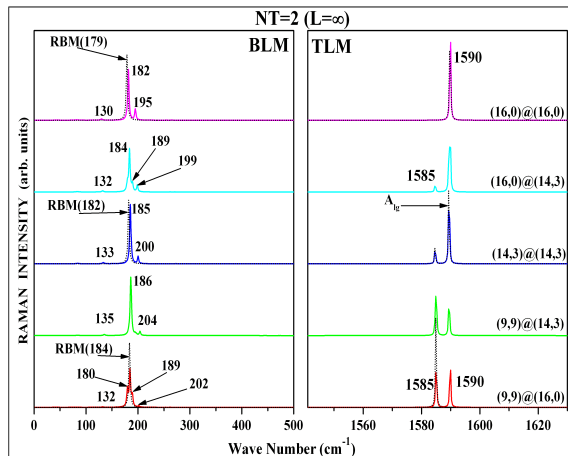


Fig. 4: the ZZ calculated Raman spectra of inhomogeneous finite BWCNT's, formed with two SWCNT's of different diameters: $(9, 9)@(n, m)$, in BLM (in the left) and TLM (in the right) ranges. Dashed lines indicate the ZZ calculated Raman spectra of corresponding SWCNT's.

IV. CONCLUSION

We have investigated Raman spectrum of homogenous and inhomogeneous bundle of SWCNT's. The analysis of results in the light of diameter and chirality dependence performed on SWCNT's samples shows a real appropriateness with our model. Thanks to the spectral moments method, we have investigated bundles consisting of more than 100 SWCNT's of several sizes. Finite size (length and number of tubes) and inhomogeneity (chirality and diameters) effects are observed essentially in the RBLM regions with additional modes which can be considered in the analysis of experimental data.

Acknowledgements

The computations were performed at CINES (Montpellier, France). The work was supported by a CNRS-France/CNRST-Morocco agreement.

BIBLIOGRAPHY

[1] S. Iijima, *nature* (London) 354, 56 (1991).
 [2] M.S. Dresselhaus and P.C. Eklund, *Adv. Phys.* 49, 705 (2000).
 [3] M.S. Dresselhaus, G. Dresselhaus, P.C. Eklund, *Science of fullerenes and carbon nanotubes*. Academic Press, New-York, (1996).
 [4] R. Saito, T. Takeya, T. Kimura, G. Dresselhaus and M. S. Dresselhaus, *Phys. Rev. B* 59, 2388 (1999).
 [5] L. Henrard, E. Hernandez, P. Bernier, and A. Rubio, *Phys. Rev. B* 60, R8521 (1999).
 [6] D. Kahn and J.P. Lu, *Phys. Rev. B* 60, 6535 (1999).

[7] J. Yu, R.K. Kalia and P. Vashishta, *J. Chem. Phys.* 103, 6697 (1995).
 [8] J. Kurti, G. Kresse, and H. Kuzmany, *Phys. Rev. B* 58, R8869 (1998).
 [9] D. Sanchez-Portal, E. Artacho, and J.M. Soler, *Phys. Rev. B* 59, 12678 (1999).
 [10] M. Milneral, J. Kurti, M. Hulman and H. Kuzmany, *Phys. Rev. B* 64, 1324 (2000).
 [11] R. Saito, T. Takeya, T. Kimura, G. Dresselhaus and M. S. Dresselhaus, *Phys. Rev. B* 57, 4145 (1998).
 [12] H. Kataura, Y. Kumazawa, Y. Maniwa, I. Umez, S. Suzuki, Y. Ohtsuka and Y. Achiba, *Synth. Met.* 103, 2555 (1999).
 [13] L. Alvarez, A. Righi, T. Guillard, S. Rols, E. Anglaret, D. Laplace, J.-L. Sauvajol, *Chem. Phys. Lett.* 316, 186 (2000).
 [14] M. A. Pimenta, A. Marucci, S. A. Empedocles, M. G. Bawendi, E. B. Hanlon, A. M. Rao, P. C. Eklund, R. E. Smalley, G. Dresselhaus, and M. S. Dresselhaus, *Phys. Rev. B* 58, R16016 (1998).
 [15] A. M. Rao, E. Richter, S. Bandow, B. Chase, P. C. Eklund, K. A. Williams, S. Fang, K. R. Subbaswamy, M. Menon, A. Thess, R. E. Smalley, G. Dresselhaus, and M. S. Dresselhaus, *Science* 275, 187 (1997).
 [16] E. Anglaret, S. Rols, J.L. Sauvajol, *Phys. Rev. Lett.* 81, 4780 (1998).
 [17] M. Lamy de la Chapelle, S. Lefrant, C. Journet, W.-K. Maser, P. Bernier, A. Loiseau, *Carbon* 36, 705-708 (1998).
 [18] M. Lamy de la Chapelle, *thèse de doctorat de l'Université de Nantes*, octobre, (1998).
 [19] A. Rahmani, J.L. Sauvajol, S. Rols and C. Benoit, *Phys. Rev. B* 66, 125404 (2002).
 [20] S. Rols, R. Almairac, L. Henrard, E. Anglaret, J.L. Sauvajol, *Eur. Phys. J. B* 10, 263 (1999).
 [21] J. C. Charlier, X. Goze, JP Michenaud, *Europhys. Lett.* 29, 43 (1995).
 [22] L. Henrard, V.N. Popov and A. Rubio, *Phys. Rev. B* 64, 205403 (2001).
 [23] A. Thess, R. Jee, P. Nikolaev, H. Dai, P. Petit, J. Robert, C. Xu, Y. Hee Lee, S. Gon Kim, AG Rinzler, DT Colbert, GE Scuseria, D. Tomanek, JE Fisher, R.E Smalley, *Science* 273, 483 (1996).
 [24] A. Rahmani, P. Jund, C. Benoit and R. Jullien, *J. Phys. Condens. Matter* 13, 5413, (2001).
 [25] C. Benoit, E. Royer and G. Poussiguet, *J. Phys.: Condens. Matter* 4, 3125 (1992).
 [26] U. D. Venkateswaran, A.M. Rao, E. Richter, M. Menon, A. Rinzler, R.E. Smalley, and P.C. Eklund, *Phys. Rev. B* 59, 10 928 (1999).
 [27] H. Ulbricht, G. Moos, and T. Hertel, *Phys. Rev. Lett.* 90, 095501 (2003).
 [28] H. Chadli, A. Rahmani, K. Sbail, P. Hermet, S. Rols, and J.-L. Sauvajol, *Phys. Rev. B* 74, 205412 (2006).
 [29] S. Guha, J. Menendez, J.B. Page, and G.B. Adams, *Phys. Rev. B* 53, 13106 (1996).
 [30] A. Rahmani, J.L. Sauvajol, J. Cambedouzou, C. Benoit, *Phys. Rev. B* 71, 125402 (2005).